Direct Computation of the PEC Body of Revolution Modal Green Function for the Electric Field Integral Equation

DOI:
10.1109/JMMCT.2022.3190789

Document status and date:
Published: 15/07/2022

Document Version:
Accepted manuscript including changes made at the peer-review stage

Direct Computation of the PEC Body of Revolution Modal Green Function for the Electric Field Integral Equation

Fahimeh Sepehripour, Martijn C. van Beurden, *Senior Member, IEEE,* Bastiaan P. de Hon

***Abstract*—We propose a five-term recurrence relation for the direct computation of the modal Green function (MGF) arising in the electric field integral equations (EFIE), when solving the scattering of PEC bodies of revolution. It is shown that, by considering it as an infinite penta-diagonal matrix, the proposed five-term recurrence relation can be solved in a stable manner in $O(M)$ steps for M modes with high and controllable accuracy. By evaluating the performance of the proposed five-term recurrence relation for several scatterers of different geometries, we show that the proposed approach enables an accurate computation with a simple algorithm.**

***Index Terms*—Electric field integral equation, Recurrence relation, Body of revolution, Modal Green function, Singularity extraction.**

I. Introduction

The electromagnetic scattering by a perfectly electric conducting (PEC) object is a classic, yet important, problem in computational electromagnetics [1], [2]. When the shape of the PEC scatterer exhibits spatial symmetry, the computational costs in evaluating the scattering can sometimes be significantly reduced. This is particularly the case for rotationally symmetric objects, called bodies of revolution (BORs) [3]–[6]. The scattering by PEC BORs has been studied since the 1960s [7]–[10]. The geometry of a BOR can be characterized using a parametric curve, known as the generating curve. The symmetry property of a BOR allows one to reduce the computational domain from a three-dimensional problem to an infinite series of decoupled two-dimensional ones.

Several approaches have been proposed to solve the scattering of PEC BORs, among which the so-called electric field integral equation (EFIE) is one of the most common methods [11], [12]. In this approach, the scattering by the BOR is formulated based on the boundary condition of the electric field at the surface of the PEC boundary, leading to a particular integral equation. EFIEs for BORs involve singular kernels, which are called modal Green functions (MGFs). While closed-form analytical solutions have been proposed for the evaluation of such singular integrals in specific cases, for instance, when the body has a slim geometry [13], the associated MGFs need to be numerically computed in general situations. Due to its singular nature, the computation of the MGFs is the most time-consuming part of the computation. Various approaches have been proposed to mitigate the computational complexities caused by such singularities. In [14], four cases are distinguished, and handled for low-order modes using a tailored combination of trapezoidal, steepest-descent-path Gauss-Hermite quadrature, Gauss-Laguerre quadrature and singularity extraction. In [15], another approach has been proposed to improve the computational efficiency of the MGF for the EFIE. The method is based on regularizing the pertaining singular integral representation for the MGF by extracting the singularity and evaluating it separately from the regular part. In particular, the regular part of the MGF is calculated utilizing the fast Fourier transform (FFT) for all modes simultaneously. The remaining singular part is then individually calculated based on a three-term recurrence relation, which leads to a significant speed up. However, this three-term term recurrence relation suffers from loss of accuracy when the source and observation points approach the axis of rotation. This issue was addressed in [16], [17] by proposing an alternative three-term recurrence relation approach that leads to more accurate results, especially when the source and observation points are close to the axis of rotation.

Despite the advantages of these singularity extraction approaches in providing high speed and accuracy, none of these methods provides a direct solution for the MGF. In fact, in all of these approaches the MGF is composed from two (or more) constituents, obtained using different methods. While there exist some direct solutions for the MGF arising in the EFIE, for example, based on various kinds of quadrature rules [10], [18], [19], these solutions are not sufficiently accurate and fast in general cases when many modes are involved.

We propose a five-term recurrence relation that allows the direct computation of all of the required MGFs arising in the EFIE at once. The proposed five-term recurrence relation is computed using a simple matrix operation that not only provides stability, but also reduces the associated computational complexity. The accuracy of the proposed technique is demonstrated by analyzing the scattering by various BORs.

II. Derivation of a 5-term recurrence relation to compute the MGF

We assume an arbitrary PEC body of revolution with an axially symmetric geometry, as shown in Fig. 1(a). Considering the symmetry of the body, embedded in a homogeneous medium, the BOR can be characterized by a planar curve (black curve in the figure), called the generating curve.

The authors are with the Department of Electrical Engineering, Eindhoven University of Technology, Eindhoven 5600 MB, The Netherlands (e-mail: f.sepehripour@tue.nl; m.c.v.beurden@tue.nl; b.p.d.hon@tue.nl.

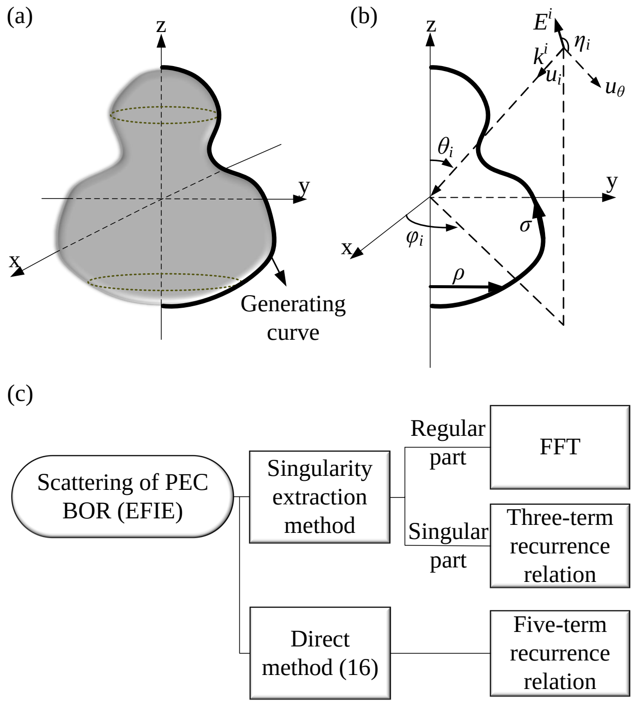

Fig. 1. Scattering analysis of PEC BOR. (a) An arbitrarily shaped PEC BOR, (b) corresponding generating curve of the BOR, (c) Top path: Indirect computational approach based on singularity extraction method involving a FFT and a three-term recurrence relation [16]. Bottom path: the proposed direct approach based on a five-term recurrence relation given in (17).

Fig. 1(b) represents the parameters of the incident field with respect to the generating curve of the BOR. The aim is to characterize the scattering of this PEC BOR based on the EFIE. One approach to compute the singular integrals arising in the MGF is based on the singularity extraction method (top path in the flow chart of Fig. 1(c)). In this method [16], the regular part of the MGF is computed based on an FFT, whereas the singular part is calculated using a three-term recurrence relation. An alternative strategy, investigated in this paper, is based on a five-term recurrence relation that avoids the decomposition of the MGF kernel (bottom path in Fig. 1(c)). In the following, the derivation of this five-term recurrence relation is explained.

We start our analysis by considering the MGF of the EFIE, denoted by g_m, expressed as

$$g_m = \int_0^{\pi} \cos(m\alpha') \frac{e^{-jkR(\alpha')}}{R(\alpha')} d\alpha', \tag{1}$$

where $m \in Z$ is the mode index of the Fourier expansion in the azimuthal direction, k is the wave number and $R(\alpha')$ is the distance between the source and observation points, defined as

$$\begin{aligned} &R(\alpha') = \sqrt{\rho^2 + \rho'^2 - 2\rho\rho'\cos\alpha' + (z-z')^2}, \\ &\alpha' = \phi - \phi'. \end{aligned} \tag{2}$$

By defining variables w and α as

$$\begin{aligned} w &= \frac{4\rho\rho'}{(\rho+\rho')^2 + (z-z')^2}, \quad 0 \le w \le 1 \\ \alpha &= \frac{\alpha' - \pi}{2}. \end{aligned} \tag{3}$$

we can express g_m as

$$g_m = (-1)^m \sqrt{\frac{w}{\rho\rho'}} F_m(w, k'), \tag{4}$$

where

$$F_m(w, k') = \int_0^{\pi/2} \cos(2m\alpha) G^E_{w,k'}(\alpha) d\alpha, \tag{5}$$

in which

$$G^E_{w,k'}(\alpha) = \frac{e^{-jk'\sqrt{1 - w\sin^2\alpha}}}{\sqrt{1 - w\sin^2\alpha}}, \tag{6}$$

and

$$k' = 2k\sqrt{\frac{\rho\rho'}{w}}. \tag{7}$$

By considering the trigonometric identity

$$\begin{aligned} \cos(2m\alpha) =& 2(1 - 2\sin^2\alpha)\cos(2(m-1)\alpha) \\ &- \cos(2(m-2)\alpha), \end{aligned} \tag{8}$$

one can write F_m as

$$\begin{aligned} F_m(w, k') = 2F_{m-1}(w, k') - F_{m-2}(w, k') - \\ 4\int_0^{\pi/2} \cos(2(m-1)\alpha)\sin^2\alpha\, G^E_{w,k'}(\alpha) d\alpha. \end{aligned} \tag{9}$$

The remaining integral on the right-hand side in (9) can be rewritten as

$$\begin{aligned} &\int_0^{\pi/2} \cos(2(m-1)\alpha)\sin^2\alpha\, G^E_{w,k'}(\alpha) d\alpha \\ &= -\frac{1}{w}\int_0^{\pi/2} \cos(2(m-1)\alpha)(1 - w\sin^2\alpha - 1) G^E_{w,k'}(\alpha) d\alpha \\ &= -\frac{1}{w}\int_0^{\pi/2} \cos(2(m-1)\alpha)(1 - w\sin^2\alpha) G^E_{w,k'}(\alpha) d\alpha \\ &+ \frac{1}{w}F_{m-1} \\ &= -\frac{1}{w}I_{m-1} + \frac{1}{w}F_{m-1}, \end{aligned} \tag{10}$$

where

$$I_m(w, k') = \int_0^{\pi/2} \cos(2m\alpha)(1 - w\sin^2\alpha) G^E_{w,k'}(\alpha) d\alpha. \tag{11}$$

By substituting (10) in (9), we have

$$\begin{aligned} F_m(w, k') =& (2 - \frac{4}{w})F_{m-1}(w, k') - F_{m-2}(w, k') + \\ &\frac{4}{w} I_{m-1}(w, k'). \end{aligned} \tag{12}$$

For $m \neq 0$, we use integration by parts (see Appendix A) to calculate I_m, leading to the equation

$$\begin{aligned} I_m(w, k') =& \frac{w}{8m}\left[F_{m-1}(w, k') - F_{m+1}(w, k')\right] - \\ &jk'\frac{w}{8m}\left[J_{m-1}(w, k') - J_{m+1}(w, k')\right], \end{aligned} \tag{13}$$

where,

$$J_m(w,k') = \int_0^{\pi/2} \cos(2m\alpha)\sqrt{1-w\sin^2\alpha}\, G^E_{w,k'}(\alpha) d\alpha. \tag{14}$$

Similarly, by applying integration by parts to $J_m(w)$ (see Appendix A) we have

$$J_m(w,k') = jk' \frac{w}{8m}\left[F_{m+1}(w,k') - F_{m-1}(w,k')\right]. \tag{15}$$

by substituting (15) and (13) in (12) we obtain

$$\left(\frac{wk'^2 m}{4(m-1)(m+1)} + 4m\frac{w-2}{w}\right) F_m = \frac{wk'^2}{8(m-1)} F_{m-2} + \\ (2m-1)F_{m-1} + (2m+1)F_{m+1} + \frac{wk'^2}{8(m+1)} F_{m+2}. \tag{16}$$

According to (4), the recurrence relation for g_m can be written as

$$\left(\frac{wk'^2}{16(m-1)(m+1)} + \frac{w-2}{w}\right) g_m = \frac{wk'^2}{32m(m-1)} g_{m-2} \\ -(\frac{1}{2} - \frac{1}{4m}) g_{m-1} - (\frac{1}{2} + \frac{1}{4m}) g_{m+1} + \frac{wk'^2}{32m(m+1)} g_{m+2}, \tag{17}$$

which is a five-term recurrence relation that holds for $m \geq 2$. Note that $m = 0$ and $m = 1$ serve as initial values. It is also worth mentioning that, since the MGF is an even function with respect to the parameter m, the relation given in (17) holds for negative integer values of m as well.

III. Exploitation of the proposed recurrence relation

It is tempting to try to exploit the 5-term recurrence relation (17) using a forward (or backward) algorithm, as is customary for three-term recurrence relations, see e.g. [20]. Fig. 2(a) and (b) illustrate the absolute error in $g_m(w)$ corresponding to the forward and backward algorithms for various values of w. Note that, for the backward recurrence relation, the difference index Δm represents the starting point of $g_{m+\Delta m}(w)$ to obtain an accurate answer for $g_m(w)$ for a fixed $m = 20$. Note further that, we used $(0, 1+j, 1-j, 1)$ as the initial points. For the purpose of numerical integration, Mathematica's NIntegrate method [21] has been used as a reference to assess the error in the modal Green functions. As observed in these figures, neither of these approaches gives rise to a stable solution for $g_m(w)$. Hence, we use a different strategy, based on a matrix equation approach [22]–[24], to compute $g_m(w)$ in (17) in a stable manner. To this end, we first represent the five-term recurrence relation as a semi-infinite penta-diagonal matrix, starting from (17) from $m = 2$, as

$$C \begin{bmatrix} g_2 \\ g_3 \\ g_4 \\ g_5 \\ g_6 \\ \vdots \\ \vdots \end{bmatrix} = \begin{bmatrix} -a_2 g_0 - b_2 g_1 \\ -a_3 g_1 \\ 0 \\ 0 \\ 0 \\ \vdots \\ \vdots \end{bmatrix}, \tag{18}$$

in which the vector with elements g_m on the left represent the unknowns and the first two modal Green functions, i.e. g_0 and g_1 are computed using global adaptive quadrature method for all values of w, except for w close to 1, i.e. $(1-w) < 10^{-12}$. For $(1-w) < 10^{-12}$, we first subtracted the integral representation of the first-kind complete elliptic integral from the MGF. Then, we computed the resulting integral using a global adaptive quadrature method.

The matrix C in (18) has the following form

$$C = \begin{bmatrix} c_2 & d_2 & e_2 & 0 & 0 & \cdots \\ b_3 & c_3 & d_3 & e_3 & 0 & \ddots \\ a_4 & b_4 & c_4 & d_4 & e_4 & \ddots \\ \vdots & \ddots & \ddots & \ddots & \ddots & \ddots \\ 0 & \cdots & \ddots & \ddots & \ddots & \ddots \end{bmatrix}, \tag{19}$$

where

$$\begin{aligned} a_m &= -\frac{wk'^2}{32m(m-1)}, \quad b_m = (\frac{1}{2} - \frac{1}{4m}), \\ c_m &= \frac{w-2}{w} + \frac{wk'^2}{16(m-1)(m+1)}, \\ d_m &= (\frac{1}{2} + \frac{1}{4m}), \qquad e_m = -\frac{wk'^2}{32m(m+1)}. \end{aligned} \tag{20}$$

In the following, we show that the infinite matrix system given in (18) can be computed in $O(M)$ steps, where M is the dimension of the corresponding truncated C matrix, i.e. $M \times M$. To this end, we decompose C into three separate matrices as follows

$$C = \frac{w-2}{w} I + \underbrace{\frac{1}{2}\begin{bmatrix} 0 & 1 & 0 & 0 & \cdots \\ 1 & 0 & 1 & 0 & \ddots \\ 0 & 1 & 0 & 1 & \ddots \\ \vdots & \ddots & \ddots & \ddots & \ddots \\ 0 & \cdots & \cdots & \cdots & \cdots \end{bmatrix}}_{C_0} +$$

$$\underbrace{\frac{1}{4}\begin{bmatrix} 1/2 & 0 & 0 & \cdots \\ 0 & 1/3 & 0 & \ddots \\ 0 & 0 & 1/4 & \ddots \\ \vdots & \ddots & \ddots & \ddots \\ 0 & \cdots & \cdots & \ddots \end{bmatrix}\begin{bmatrix} 0 & 1 & 0 & \cdots \\ -1 & 0 & 1 & \ddots \\ 0 & -1 & 0 & \ddots \\ \vdots & \ddots & \ddots & \ddots \\ 0 & \cdots & \ddots & \ddots \end{bmatrix}}_{C_1} +$$

$$\underbrace{wk'^2 \begin{bmatrix} c'_{2,2} & 0 & e'_2 & 0 & \cdots \\ 0 & c'_{3,2} & 0 & e'_3 & \ddots \\ a'_4 & 0 & c'_{4,2} & 0 & \ddots \\ \vdots & \ddots & \ddots & \ddots & \ddots \\ 0 & \cdots & \cdots & \cdots & \ddots \end{bmatrix}}_{C_2}, \tag{21}$$

in which I is the identity matrix and

$$\begin{aligned} a'_m &= -\frac{1}{32m(m-1)}, \\ c'_{m,2} &= \frac{1}{16(m-1)(m+1)}, \\ e'_m &= -\frac{1}{32m(m+1)}. \end{aligned} \tag{22}$$

In (21), C_0, C_1 and C_2 are all independent of w and k' and can be set up once and for all once a fixed finite dimension has been chosen. Below, we explain why the infinite matrix can be truncated to a finite dimension.

A. Solvability of the static part of the MGF

We note that the matrix $[(w-2)/w]I + C_0 + C_1$ corresponds to the recurrence relation for the static part of the modal Green function obtained in [16]. For $0 < w < 1$, this matrix is diagonally dominant and, as a result, non-singular and invertible. In [16], a combined forward/backward three-term recurrence relation algorithm was proposed, enabling fast, accurate and stable computation of the static part of the MGF. For the special case $w = 1$, we first concentrate on $[(w-2)/w]I + C_0$, i.e. without C_1, that can be represented

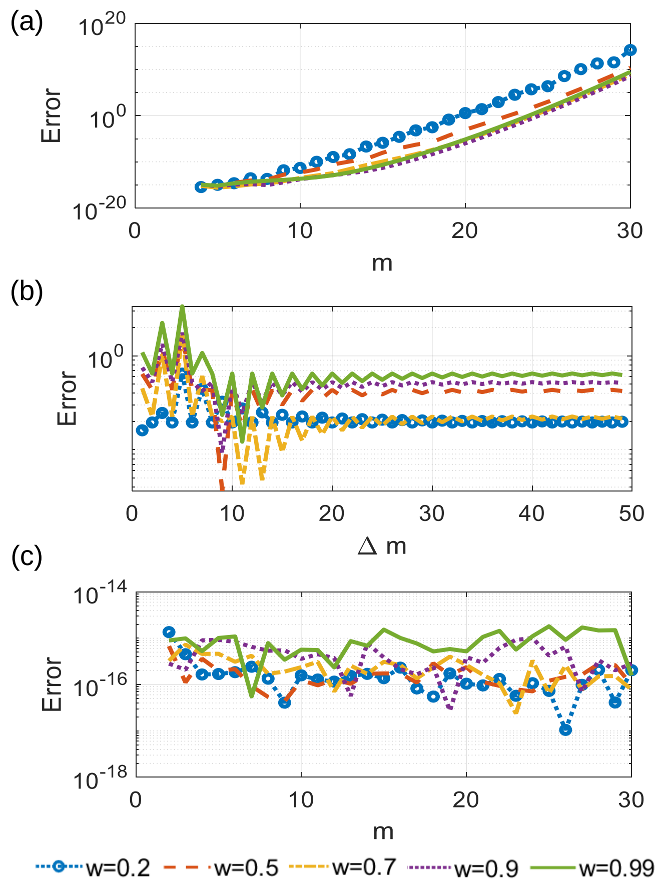

Fig. 2. Computation error of $g_m(w)$ for $w = 0.2, 0.5, 0.7, 0.9, 0.99$, $k = 2\pi$, $\rho = 1.1$ and $\rho' = 1.7$ using, (a) forward recurrence relation, (b) backward recurrence relation, (c) penta-diagonal matrix approach.

as

$$\begin{bmatrix} -1 & \frac{1}{2} & 0 & 0 & \cdots \\ \frac{1}{2} & -1 & \frac{1}{2} & 0 & \ddots \\ 0 & \frac{1}{2} & -1 & \frac{1}{2} & \ddots \\ \vdots & \ddots & \ddots & \ddots & \ddots \\ 0 & \cdots & \cdots & \cdots & \cdots \end{bmatrix}\begin{bmatrix} g_2 \\ g_3 \\ g_4 \\ g_5 \\ \vdots \\ \vdots \end{bmatrix} = \begin{bmatrix} -\frac{1}{2}g_1 \\ 0 \\ 0 \\ 0 \\ \vdots \\ \vdots \end{bmatrix}. \tag{23}$$

This is a familiar matrix that arises from a finite-difference approximation of a second-order derivative. In this matrix the diagonal elements are equal to -1. At the same time, the row-wise sums of the absolute values from the lower and upper diagonal elements are equal to 1. Therefore, the matrix is no longer diagonally dominant. By analysing the matrix equation in (23) from the second row onward by means of a z transformation, which is feasible owing to the constant coefficients along the diagonal of $[(w-2)/w]I + C_0$, one obtains the following two eigenvectors with eigenvalue zero

$$v_1 = \begin{bmatrix} 1 \\ 1 \\ 1 \\ \vdots \\ \vdots \end{bmatrix}, \quad v_2 = \begin{bmatrix} 1 \\ 2 \\ \vdots \\ m \\ \vdots \end{bmatrix}, \tag{24}$$

which is consistent with the discretization of a second order-derivative. The vector v_2 is not a desired solution since its elements are linearly increasing with m and is therefore not a minimal solution. Consequently, v_1 is the solution of interest. Additionally, we note that v_1 is also an eigenvector of C_1 with eigenvalue zero, apart from the first row. In spite of the singular nature of the functions $g_m(w)$ for $w = 1$, it is still possible to solve for the coefficients g_m/g_1 with the help of v_1 and the first row of $[(w-2)/w]I + C_0 + C_1$, i.e.

$$\frac{1}{g_1} \begin{bmatrix} g_2 \\ g_3 \\ g_4 \\ g_5 \\ \vdots \\ \vdots \end{bmatrix} = \frac{3}{4} v_1, \tag{25}$$

which leads to an acceptable and stable solution for the static case for $w = 1$, in part owing to the particular form of the right-hand side of the equation.

B. Solvability of the entire MGF

The last two matrices in (21), namely C_1 and C_2, are Hilbert-Schmidt and therefore compact (see Appendix B). Therefore, for $0 \leq w < 1$, the penta-diagonal matrix C in (18) is the summation of the invertible matrix $[(w-2)/w]I + C_0$ and the compact matrix $C_1 + C_2$. For such a case, it is known that the infinite matrix can be truncated to finite dimension, M, as a special case of a projection method [26], [27], to yield a convergent algorithm. The resulting finite matrix equation can then be solved in $O(M)$ steps, owing to the banded nature of the matrix.

Fig. 2(c) indicates the corresponding absolute error for several values of w, when the matrix relation of (18) is used to compute the sequence $g_m(w)$, where the infinite matrix in (18) was truncated to a 100×100 matrix. For computing the associated integrals as an independent reference, Mathematica's NIntegrate method was employed. It is observed that, as opposed to the forward and backward algorithms, the latter approach provides a stable solution with an error level that is around machine precision.

IV. Numerical Results

To evaluate the applicability of the proposed five-term recurrence relation method for characterizing the scattering by PEC BORs, we analyze the scattering of PEC objects with two different shapes namely a sphere and a torus. We discretized the surface currents on the generating curve of BOR in the tangential direction, indicated by σ in Fig. 1 (a) using basis functions that are piece-wise linear for σ directed currents and piecewise constant for the ϕ directed currents. The computation was performed using MATLAB 2019b on a laptop with 16 GB of RAM and an Intel core i7-8850H processor. We start by considering the case of a PEC sphere, embedded in free space. The radius of the sphere is assumed to be $r/\lambda = 1$, where λ is the free-space wavelength. In the computation, the generating curve is discretized with 40 segments. We assume that the angle of incidence is $\theta_i = 0$ and $\phi_i = 0$.

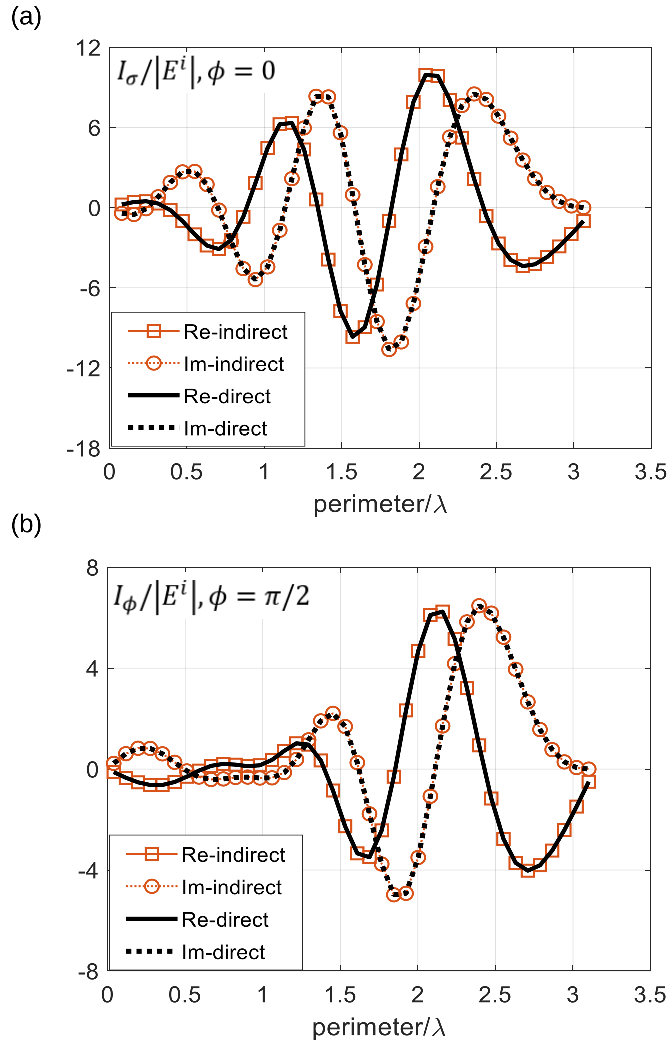

Fig. 3. Scattering analysis of a perfectly conducting sphere with the radius $r/\lambda = 1$, for a θ-polarized incident wave. (a) Surface current in tangential direction in the plane $\phi = 0$, obtained from the proposed five-term recurrence relation (black) and from the singularity extraction method [16] (orange). The induced currents are plotted over the perimeter of the generating curve, normalized to the wavelength (i.e. the parameter perimeter/λ). (b) Same as (a) but for ϕ-directed surface current in the plane $\phi = \pi/2$.

Fig. 3 (a) and (b) illustrate the induced tangential (I_σ) and ϕ-directed (I_ϕ) surface currents in the planes $\phi = 0$ and $\phi = \pi/2$ respectively, for a θ-polarized incident plane wave. The induced currents are plotted versus the perimeter

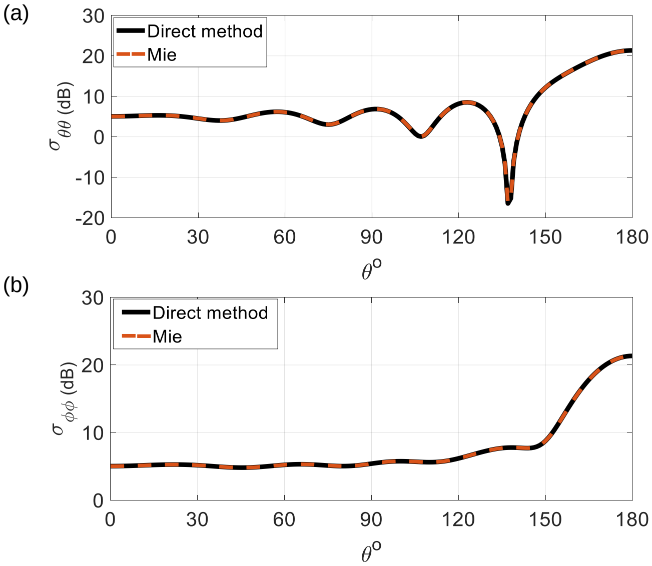

Fig. 4. Bistatic RCS of a PEC sphere with radius of $r/\lambda = 1$, and $k = 2\pi$. (a) $\theta\theta$ component of the RCS in $\phi_{obs} = 0$, obtained from the proposed method (solid black curve) and Mie series (dashed orange curve) [25]. (b) Same as (a) but for the $\phi\phi$ component of the RCS.

of the generating curve, normalized to the wavelength (i.e. the parameter perimeter/λ). The results are calculated based on the proposed direct method (black) and the singularity extraction method (orange) [16]. As seen, the results match each other in both cases (the maximum absolute error between the results is 10^{-8}), confirming the accuracy of the proposed method. It should be noted that, when using the three-term recurrence relation method proposed in [16] (the indirect approach), it is only the singular part of MGF that is computed and the computation of the remaining part, i.e. the regular part of the MGF, remains as extra work that includes the sampling of the 3D Green function. By contrast, the proposed five-term recurrence relation directly yields the entire sequence of MGFs. For further verification of the proposed approach, we calculate the bistatic radar cross-section (BRCS) corresponding to the θ and ϕ polarizations at the observation plane $\phi = 0$. Fig. 4 represents $\sigma_{\theta\theta}$ and $\sigma_{\phi\phi}$, obtained from our method (solid black curve) and compared to an independent reference, namely Mie scattering solution (dashed orange line) [25]. The results of this figure, which are also consistent with the previously reported results in the literature [28], provides more evidence for the validity of the proposed method (the maximum relative error in panels (a) and (b) are 0.03 and 0.003, respectively).

The proposed approach can also be employed to analyze the scattering by other kinds of bodies. As an example, we consider a closed PEC BOR of torus shape with the minor and major radii of $r_1/\lambda = 3.33 \times 10^{-5}$ and $r_2/\lambda = 10^{-4}$ as depicted in Fig. 5(a). We assume the frequency and the incident angle of the incident field to be $f = 100$ kHz and $\theta_i = 0$, respectively. Similar to the previous case, the number of discretized segments over the generating curve is considered to be 40. Shown in Fig. 5(b) is the associated $\theta\theta$ component of the bistatic RCS (black solid curve), which is compared to the result provided in the literature [28] (orange

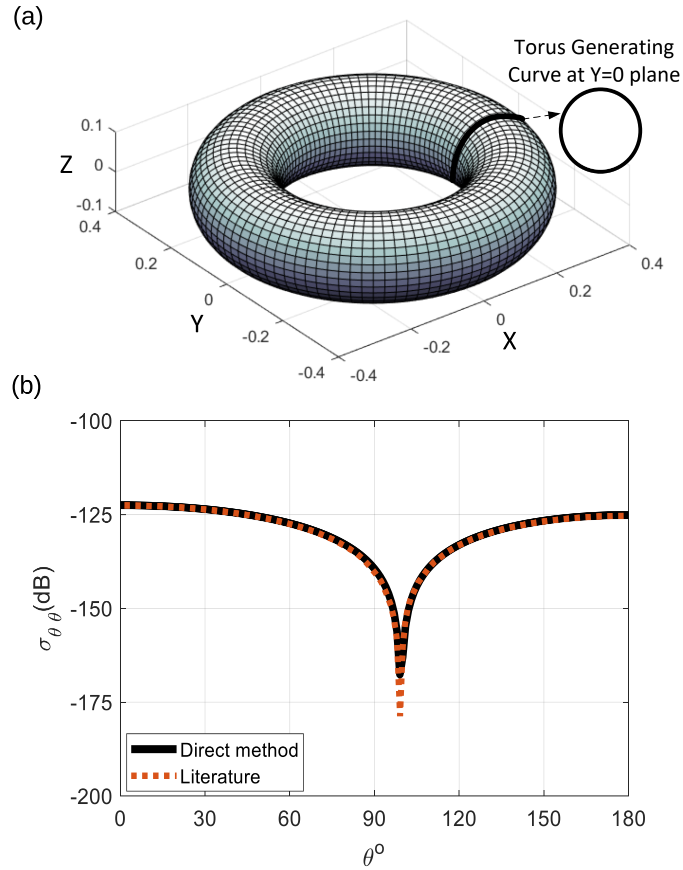

Fig. 5. Far-field analysis of a perfectly conducting torus for a θ-polarized incident wave at the frequency $f = 100$ kHz. (a) Torus with the minor and major radii of $r_1/\lambda = 3.33 \times 10^{-5}$ and $r_2/\lambda = 10^{-4}$. (b) $\theta\theta$ component of the bistatic RCS of the PEC torus discussed before, obtained from the proposed method (solid back curve) and the literature [28] (dashed orange curve).

dashed line). As a third example, we consider a PEC circular cylinder of radius $r/\lambda = 2$ and height $h/\lambda = 2$. Fig. 6(a) shows the current in the tangential direction in the plane $\phi = 0$, upon considering a θ-polarized incident field with an angle of incidence $\theta_i = \pi/4$. The results are obtained based on the proposed direct five-term recurrence relation (black), and the three-term recurrence relation approach (orange). The corresponding ϕ-directed currents at $\phi = \pi/2$ are illustrated in Fig. 6(b).

The comparison of the proposed five-term recurrence relation with the three-term recurrence relation cross validates the performance of the proposed method. It is more interesting to compare the computational characteristics of the two different approaches. In Table I, we have compared the computational characteristics (computation time, maximum difference between direct and indirect approaches, and number of required modes) of the proposed method with the singularity extraction method proposed in [16]. For calculating the number of required modes, we assumed an oblique incidence angle of $\theta_i = \pi/4$, while neglecting the spectral content of incident fields possessing amplitudes less than 10^{-14}. As observed in this table, the difference between the indirect and direct approaches is small, yet, the proposed direct method offers a

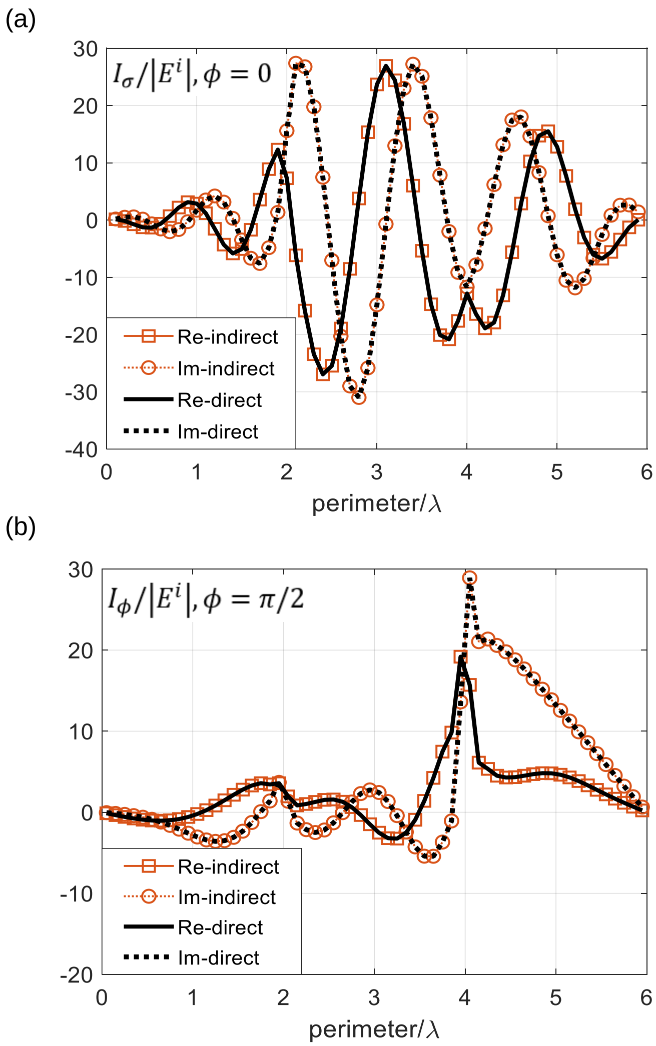

Fig. 6. Scattering analysis of a perfectly conducting cylinder with the radius $r/\lambda = 2$, and $h/\lambda = 2$ for a θ-polarized incident wave. (a) Surface current in tangential direction in the plane $\phi = 0$, obtained from the proposed five-term recurrence relation (black), from the singularity extraction method [16]. (b) Same as (a) but for ϕ-directed surface current in the plane $\phi = \pi/2$.

shorter computation time for both sphere and cylinder cases.

Finally, it is worth investigating the effect of the BOR size on the computational characteristics. To this end, we consider the scattering by PEC spheres of different sizes, namely $r/\lambda = 5$, $r/\lambda = 10$, $r/\lambda = 20$. Table II provides the information regarding the computational features corresponding to all of the aforementioned cases, including the computation time, the minimum number of modes required for convergence, and the corresponding computational error, i.e. maximum difference in computing the MGF between the proposed method and Integral of Matlab. It is observed that, by increasing the size of the BOR, one also needs to increase the number of modes that is taken into account to maintain the same accuracy, which in turn increases the computation time. In addition, the computation times depend quadratically on the number of segments due to the dense matrix method we employ in our current implementation. The computation time of the MGF using the proposed five-term recurrence

TABLE I
COMPUTATIONAL CHARACTERISTICS OF DIFFERENT BORS INVESTIGATED IN THE PAPER

Object	Sphere (Fig. 3)	Cylinder (Fig. 6)
Perimeter of generating curve	$\pi\lambda$	6λ
Number of segments	40	60
Number of modes	22	30
Total computation time (direct method) (sec)	224	380
Total computation time (indirect method) (sec)	250	398
Maximum difference of the induced currents between the direct and indirect methods	10^{-8}	7×10^{-8}

relation is also compared with the indirect method (three-term recurrence relation approach together with FFT for the regular part) proposed in [16]. As can be seen in Tables I–II, for small bodies the direct method results in shorter computation times. Yet, by increasing the size of the BOR, the computation time of the direct approach becomes longer than for the indirect one. The main reason is that in the direct method, the computational costs of the initial values (computation of integrals for the dynamic Green function) become dominant for larger bodies. On the other hand, in the indirect method, the computation of the initial values is faster owing to the static Green function being used.

V. CONCLUSION

We have proposed a direct approach for computing the MGF arising in the EFIE, when solving the electromagnetic scattering of bodies of revolution. To this end we derived a five-term recurrence relation for the MGF. It turns out that forward or backward evaluation of the recurrence relation are not stable procedures. However, we have shown that a penta-diagonal matrix approach is demonstrably stable, and for M MGFs can be performed in $O(M)$ complexity. Moreover, our proposed direct method is simple, as opposed to the indirect (heterogeneous) methods involving the extraction of the static Green function. We have validated our approach numerically, through scattering simulations for a PEC sphere and a PEC torus. The maximum absolute error in computing the MGFs through the five-term recurrence relation was 10^{-14}.

APPENDIX A
INTEGRATION BY PARTS TO $I_m(w, k')$

Here, we derive (13) using the integration by parts

$$\begin{aligned}
I_m(w,k') &= \int_0^{\pi/2} \cos(2m\alpha)(1 - w\sin^2\alpha) G^E_{w,k'}(\alpha) d\alpha \\
&= \frac{1}{2m}\left[\sin(2m\alpha)(1 - w\sin^2\alpha) G^E_{w,k'}(\alpha)\right]_0^{\pi/2} \\
&+ \frac{w}{4m}\int_0^{\pi/2} \sin 2\alpha \sin(2m\alpha) G^E_{w,k'}(\alpha) d\alpha \\
&- jk'\frac{w}{4m}\int_0^{\pi/2} \sin 2\alpha \sin(2m\alpha)\sqrt{1 - w\sin^2\alpha}\, G^E_{w,k'}(\alpha) d\alpha,
\end{aligned} \tag{26}$$

TABLE II
COMPUTATIONAL CHARACTERISTICS OF SCATTERING OF PEC SPHERES WITH DIFFERENT SIZES

Object	Sphere 1	Sphere 2	Sphere 3
Perimeter of generating curve	$5\pi\lambda$	$10\pi\lambda$	$20\pi\lambda$
Number of segments	40	80	160
Number of modes	53	80	135
Computation time of MGF using Integral of Matlab (sec)	1093	7579	58331
Total computation time of MGF using indirect method (sec)	101	358	1875
Computation time of initial values (the first and last two modes) for MGF using direct method (sec)	80	347	1889
Computation time of setting up and solving the penta-diagonal matrix for MGF using direct method (sec)	3	38	363
Total computation time of MGF using direct method (sec)	83	385	2252
Total computation time of scattering problem (sec)	248	1001	7468
Maximum difference in computing MGF, between the proposed method and Integral of Matlab	6×10^{-12}	7×10^{-12}	7×10^{-11}

and the trigonometry formula

$$\sin 2\alpha \sin(2m\alpha) = \frac{1}{2}(\cos(2(m-1)\alpha) - \cos(2(m+1)\alpha)). \tag{27}$$

This results in (13).

INTEGRATION BY PARTS TO $J_m(w,k')$

Similar to $I_m(w,k')$, we also subject $J_m(w,k')$ to integration by parts

$$\begin{aligned} J_m(w,k') &= \int_0^{\pi/2} \cos(2m\alpha)\sqrt{1-w\sin^2\alpha}\, G^E_{w,k'}(\alpha)d\alpha \\ &= \int_0^{\pi/2} \cos(2m\alpha) e^{-jk'\sqrt{1-w\sin^2\alpha}} d\alpha \\ &= \frac{1}{2m}\left[\sin(2m\alpha)e^{-jk'\sqrt{1-w\sin^2\alpha}}\right]_0^{\pi/2} - \\ & jk'\frac{w}{4m}\int_0^{\pi/2} \sin 2\alpha \sin(2m\alpha) G^E_{w,k'}(\alpha)d\alpha. \end{aligned} \tag{28}$$

and use (27) to arrive at (15).

APPENDIX B

For an infinite matrix operator in ℓ^2, the sufficient condition for compactness of a matrix with $[a_{ij}]$ elements is [29]

$$\sum_{i=1}^{\infty}\sum_{j=1}^{\infty} |a_{ij}|^2 < \infty. \tag{29}$$

In C_1 in (21), only the first lower and upper diagonal elements are non-zero, being equal to $-\frac{1}{4m}$ and $\frac{1}{4m}$, respectively. As a results, it can be easily shown that this matrix satisfies the sufficient condition of compactness in (29)

$$\begin{aligned} \sum_{i=1}^{\infty}\sum_{j=1}^{\infty} |a_{ij}|^2 =& \frac{1}{8} + \sum_{m=3}^{\infty} |a_{m,m-1}|^2 + |a_{m,m+1}|^2 \\ &= \frac{1}{8}(1 + \sum_{m=3}^{\infty}\frac{1}{m^2}) \end{aligned} \tag{30}$$

which is convergent according to Basel problem [30], proving the compactness of C_1.
Now we investigate the compactness of C_2. We show that the matrix C_2 in (21) satisfies (29).

$$\begin{aligned} \sum_{i=1}^{\infty}\sum_{j=1}^{\infty} |a_{ij}|^2 =& |c'_{2,2}|^2 + |e'_2|^2 + |c'_{3,2}|^2 + |e'_3|^2 + \\ & \sum_{m=4}^{\infty} |a'_m|^2 + |c'_{m,2}|^2 + |e'_m|^2, \end{aligned} \tag{31}$$

in which a'_m, $c'_{m,2}$ and e'_m are defined in (22). The first four terms in the right hand side of (31) are finite. It can be shown that the last term in this equation (the series) is convergent. By employing the parameters defined in (22), the series can be rewritten as

$$\begin{aligned} & \sum_{m=4}^{\infty} |a'_m|^2 + |c'_{m,2}|^2 + |e'_m|^2 = \\ & \frac{2}{32^2}\sum_{m=4}^{\infty}\left[\frac{1}{(m-1)^2} + \frac{1}{m^2} + \frac{1}{(m+1)^2} - \frac{3}{(m-1)(m+1)}\right], \end{aligned} \tag{32}$$

in which the first three terms are convergent according to Basel problem. The last term of the series can be expressed as

$$\sum_{m=4}^{\infty}\left(\frac{1}{(m-1)} - \frac{1}{(m+1)}\right) = \frac{1}{3} + \frac{1}{4}, \tag{33}$$

which is again a convergent series.These features represent that C_2 in (21) satisfy the sufficient condition of compactness. As such, C_1 and C_2 are Hilbert-Schmidt operators with finite absolute norm [31], enabling the truncation of each of them to an $M \times M$ matrix [26], [27].

ACKNOWLEDGMENT

This research was supported by the NWO-TTW HTSM project MAX META-XT, under project number 16184.

REFERENCES

[1] A. Glisson and D. Wilton, "Simple and efficient numerical methods for problems of electromagnetic radiation and scattering from surfaces," *IEEE Trans. Antennas Propag.*, vol. 28, no. 5, pp. 593–603, 1980.

[2] S. Rao, D. Wilton, and A. Glisson, "Electromagnetic scattering by surfaces of arbitrary shape," *IEEE Trans. Antennas Propag.*, vol. 30, no. 3, pp. 409–418, 1982.

[3] C. L. Epstein, L. Greengard, and M. O'Neil, "A high-order wideband direct solver for electromagnetic scattering from bodies of revolution," *J. Comput. Phys.*, vol. 387, pp. 205–229, 2019. [Online]. Available: https://www.sciencedirect.com/science/article/pii/S0021999119301585

[4] J. Helsing and A. Karlsson, "An extended charge-current formulation of the electromagnetic transmission problem," *SIAM J. Appl. Math.*, vol. 80, no. 2, pp. 951–976, 2020. [Online]. Available: https://doi.org/10.1137/19M1286803

[5] J. Helsing and A. Rosén, "Dirac integral equations for dielectric and plasmonic scattering," *Integral Equ. Oper. Theory*, vol. 93, no. 5, p. 48, 2021. [Online]. Available: https://doi.org/10.1007/s00020-021-02657-1

[6] J. Helsing, A. Karlsson, and A. Rosén, "Comparison of integral equations for the Maxwell transmission problem with general permittivities," *Adv. Comput. Math.*, vol. 47, no. 5, p. 76, 2021. [Online]. Available: https://doi.org/10.1007/s10444-021-09904-4

[7] M. Andreasen, "Scattering from bodies of revolution," *IEEE Trans. Antennas Propag.*, vol. 13, no. 2, pp. 303–310, 1965.

[8] J. R. Mautz and R. Harrington, "Radiation and scattering from bodies of revolution," *Appl. Sci. Res.*, vol. 20, no. 1, pp. 405–435, 1969.

[9] A. W. Glisson and D. R. Wilton, "Simple and efficient numerical techniques for treating bodies of revolution," MISSISSIPPI UNIV UNIVERSITY, Tech. Rep., 1979.

[10] A. A. Mohsen and A. K. Abdelmageed, "A fast algorithm for treating em scattering by bodies of revolution," *AEU - Int. J. Electron. Commun.*, vol. 55, no. 3, pp. 164–170, 2001.

[11] S. Gedney and R. Mittra, "The use of the FFT for the efficient solution of the problem of electromagnetic scattering by a body of revolution," in *1988 IEEE AP-S. Int. Symp., Antennas Propag.*

[12] M. Tong and W. Chew, "Evaluation of singular fourier coefficients in solving electromagnetic scattering by body of revolution," *Radio Sci.*, vol. 43, no. 04, pp. 1–9, 2008.

[13] W. M. Yu, D. G. Fang, and T. J. Cui, "Closed form modal Green's functions for accelerated computation of bodies of revolution," *IEEE Trans. Antennas Propag.*, vol. 56, no. 11, pp. 3452–3461, 2008.

[14] M. Gustafsson, "Accurate and efficient evaluation of modal Green's functions," *J. Electromagn. Waves Appl.*, vol. 24, no. 10, pp. 1291–1301, 2010.

[15] S. D. Gedney and R. Mittra, "The use of the FFT for the efficient solution of the problem of electromagnetic scattering by a body of revolution," *IEEE Trans. Antennas Propag.*, vol. 38, no. 3, pp. 313–322, 1990.

[16] J. A. H. M. Vaessen, M. C. van Beurden, and A. G. Tijhuis, "Accurate and efficient computation of the modal Green's function arising in the electric-field integral equation for a body of revolution," *IEEE Trans. Antennas Propag.*, vol. 60, no. 7, pp. 3294–3304, 2012.

[17] J. A. H. M. Vaessen, "Efficient modeling of electromagnetic fields in stochastic configurations," Ph.D. dissertation, Technische Universiteit Eindhoven, 2015.

[18] A. Abdelmageed, "Efficient evaluation of modal Green's functions arising in em scattering by bodies of revolution," *Prog. Electromagn. Res.*, vol. 27, pp. 337–356, 2000.

[19] Ú. C. Resende, F. J. Moreira, and O. M. Pereira-Filho, "Efficient evaluation of singular integral equations in moment method analysis of bodies of revolution," *J. Microw. Optoelectron. Electromagn. Appl.*, vol. 6, no. 2, pp. 373–391, 2007.

[20] W. H. Press, W. T. Vetterling, S. A. Teukolsky, and B. P. Flannery, *Numerical recipes*. Cambridge university press Cambridge, 1986, vol. 818.

[21] "Wolfram Research, NIntegrate, Wolfram Language function," 1988. [Online]. Available: https://reference.wolfram.com/language/ref/NIntegrate.html

[22] J. W. Miller, "A matrix equation approach to solving recurrence relations in two-dimensional random walks," *J. Appl. Probab.*, vol. 31, no. 3, pp. 646–659, 1994.

[23] R. B. Taher and M. Rachidi, "Linear recurrence relations in the algebra of matrices and applications," *Linear Algebra Appl.*, vol. 330, no. 1-3, pp. 15–24, 2001.

[24] G.-S. Cheon, S.-G. Hwang, S.-H. Rim, and S.-Z. Song, "Matrices determined by a linear recurrence relation among entries," *Linear Algebra Appl.*, vol. 373, pp. 89–99, 2003.

[25] Giannakopoulos, Ilias, "Matlab software for the Mie scattering of PEC and homogeneous spheres irradiated by a linearly polarized plane wave," 2018. [Online]. Available: https://www.github.com/GiannakopoulosIlias/MieScattering

[26] R. Kress, V. Maz'ya, and V. Kozlov, *Linear Integral Equations*. Springer, 1989, vol. 82.

[27] D. A. Miller, "An introduction to functional analysis for science and engineering," *arXiv preprint arXiv:1904.02539*, 2019.

[28] Q. S. Liu, S. Sun, and W. C. Chew, "A potential-based integral equation method for low-frequency electromagnetic problems," *IEEE Trans. Antennas Propag.*, vol. 66, no. 3, pp. 1413–1426, 2018.

[29] G. W. Hanson and A. B. Yakovlev, *Operator theory for electromagnetics: an introduction*. Springer Science & Business Media, 2013.

[30] R. Ayoub, "Euler and the zeta function," *Amer. Math. Monthly.*, vol. 81, no. 10, pp. 1067–1086, 1974.

[31] M. Renardy and R. C. Rogers, *An introduction to partial differential equations*. Springer Science & Business Media, 2006, vol. 13.